Benchmark of convolution and deconvolution models: implications for planetary opposition surges

E. Déau*,[1], A. Brahic[2], L. Dones[3], and C.C. Porco[4]

[1]*Jet Propulsion Laboratory, NASA/CalTech, 4800 Oak Grove Drive Pasadena CA 91109, U.S.A.*
[2]*Université Denis Diderot, Laboratoire AIM, 10 rue A. Domon et L. Duquet, 75205 Paris, France.*
[3]*Southwest Research Institute, 1050 Walnut Street, Suite 300, Boulder CO 80302, U.S.A.*
[4]*CICLOPS, 3100 Walnut Street, Suite A535, Boulder CO 80303, U.S.A.*

We benchmark several convolution and deconvolution models on phase curves at small phase angles (0.005°-1°). These curves were provided by several NASA missions (Clementine/UVVIS, Galileo/SSI and Cassini/ISS) when the Sun had different angular radii ($\alpha_\odot$=0.266°, 0.051°, 0.028°). For the smallest phase angles, the brightness of the objects (Moon, Europa and the Saturn's rings) exhibits a strong flattening below the angular size of the Sun. However, the brightness continues to increase below $\alpha_\odot$ before finally flattening at $0.4\alpha_\odot$. These behaviors are consistent with the convolution models tested.

INTRODUCTION

When the observer and the source of light are aligned, a strong surge called the opposition effect is observed in the phase curves of astronomical objects [1]. Although observed since the 19th century, the opposition effect is not understood and the causes which provoke it are still a matter of debate [1]. Several theoretical models have proposed to explain the shape of the surge by different mechanisms [2, 3]. Because the Sun is not a point-like light source for Solar System objects, it is therefore necessary to deconvolve the data or to convolve the theoretical models. Both approaches are tested on phase curves at small phase angles.

OPPOSITION DATA

We use the opposition data of the Moon observed by Clementine/UVVIS [4], Europa seen by Galileo/SSI [5] and the Saturn's rings observed by Cassini/ISS in 2005 [6].

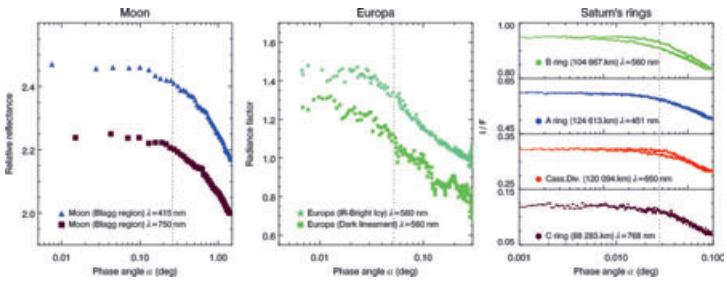

Figure 1. Phase curves of the Moon, Europa and the Saturn's rings from images of Clementine, Galileo and Cassini. Vertical dotted lines correspond to solar angular radii.

*Corresponding author: Estelle Deau (estelle.deau@jpl.nasa.gov)

CONVOLUTION MODELS

We tested two convolution models. The first one is the limb darkening function of [7]: $W(\mu') = a_\lambda + b_\lambda \mu' + c_\lambda \left[1 - \mu' \cdot \log\left(1 + 1/\mu'\right)\right]$, where $\mu' = \cos\theta'$ and θ' varies from 0 to the Sun's angular radius $\alpha_\odot$. a_λ, b_λ and c_λ are coefficients that depend on the wavelength. It has been used in the past to be convolved with a theoretical opposition effect function of [8]. The normalized convolution of the linear-exponential function of [9] $r_{linexp}(\alpha) = I_b + I_s \cdot \alpha + I_p \cdot \exp\left(-\alpha/2w\right)$ to the limb darkening function is:

$$r_{pw}(\alpha) = \frac{\int_0^{\alpha_\odot} d\theta' \int_0^{2\pi} d\phi' \sin\theta' r_{linexp}(\alpha) \cdot W(\cos\theta') \cos\theta_0(\Omega')}{\int_0^{\alpha_\odot} d\theta' \int_0^{2\pi} d\phi' \sin\theta' W(\cos\theta') \cos\theta_0(\Omega')}. \quad (1)$$

The angles θ_0, Ω' and ϕ' are fully described in [8]. The second limb darkening function tested here is the one-parameter solar limb-darkening model of [10]: $I_\lambda(\hat{r}) = (1 - \hat{r}^2)^{\beta_\lambda}$ where $I_\lambda(\hat{r})$ is the normalized limb-darkened solar intensity, $\hat{r}$ is the normalized radial coordinate of the solar disk, and β_λ is a wavelength-dependent constant. We fitted the linear exponential function to the data and computed r_{hm} by using:

$$r_{hm}(\alpha) = \frac{\int r_{linexp}(\alpha, \Omega) I_\lambda(\Omega) d\Omega}{\int I_\lambda(\Omega) d\Omega} \quad (2)$$

where $I_\lambda(\Omega)$ is the limb-darkened solar intensity, $\alpha(\Omega)$ is the phase angle, and the integrations were made over the solid angle $d\Omega$ of the solar disk.

As a result, both convolution models tested here give a good agreement with the data and between themselves (Fig. 2).

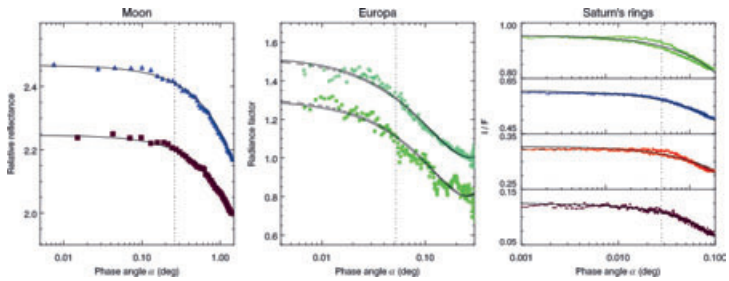

Figure 2. Phase curves of the Moon, Europa and the Saturn's rings fitted with the model of [7] in solid curves and the model of [10] in dashed curves.

DECONVOLUTION MODEL

We performed previously a convolution of the linear-exponential function to several limb darkening functions. However, this refinement does not provide information about the behavior of the brightness if the Sun were a point-like source, because the linear-exponential function intrinsically flattens as $\alpha \to 0$ (see dashed curve in Fig. 3). Few models that deconvolve phase curves exist so we use a simple model. The deconvolution model of [11] uses the logarithmic function of [12] because it does not flatten at small phase angles and

assumes a logarithmic increase of the data below the light source's angular size, as for larger phase angles:

$$r_{log}(\alpha) = a_0 + a_1 \cdot \ln(\alpha) \quad (3)$$

This assumption is consistent with the recent laboratory measurements of [13] at small phase angles (0.008^o –1.51^o), that did not show any flattening of the phase curves (Fig. 3). This is because [13] increase the laser separation distance from 25 meters to 40 meters to obtain the smallest phase angles and then, artificially decrease the angular size of their light source.

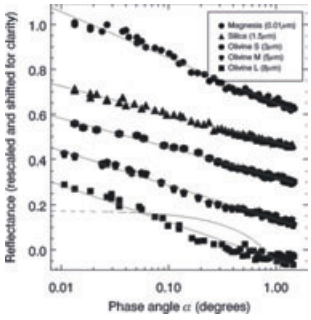

Figure 3. Laboratory phase curves of [13] at very small phase angles

DISCUSSION

Morphology of the surge before and after the deconvolution

With the convolution and deconvolution models, the behavior of the surge appears to be more clear. The flattening of the phase curves is progressive and effective at approximately $0.4\alpha_{\odot}$. This value is found either with the phase curves (Fig. 4) or either by looking at the derivative of the convolved linear-exponential function fitted to the data. The deconvolution model suggests a logarithmic trend for the brightness for α near 0^o.

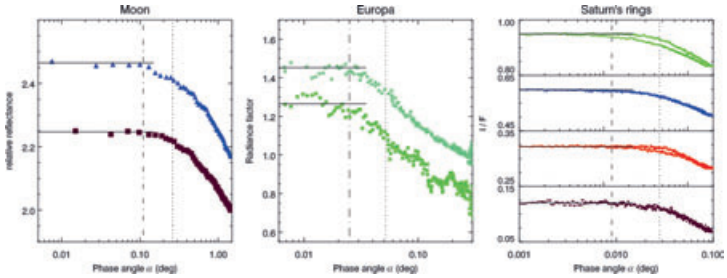

Figure 4. Phase curves of the Moon, Europa and the Saturn's rings fitted with several logarithmic functions of [12]. Vertical dotted lines correspond to α of effective flattening.

Implication for the surge of planetary surfaces

We tested the influence of the solar angular size by representing in Fig. 5 the convolved and deconvolved angular width of the surge as a function of the distance from the Sun (in Astronomical Units) for various Solar System objects [11]. The convolved HWHMs follow a power-law function with the heliocentric distance while the deconvolved HWHMs are independent of the distance from the Sun (see Fig. 5). With the deconvolved HWHMs, Solar System objects seem to be grouped by their albedo. This could be a consequence of the opposition effect mechanisms, since they are albedo-dependent [2, 3].

CONCLUSION

To better understand the behavior of the brightness near the solar angular radius, we (1) convolved the theoretical models and (2) deconvolved the data. The first approach shows a

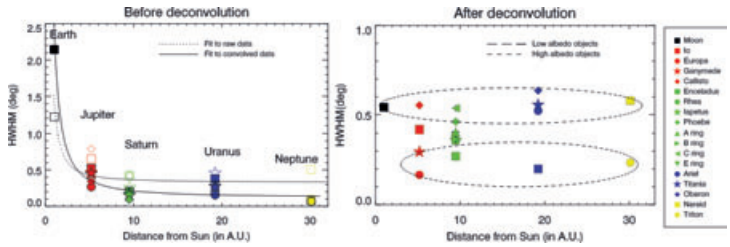

Figure 5. Angular width of the surge before and after the deconvolution for various rings and satellites of the Solar System from the study of [11].

good agreement between the two convolution models used and the second approach finds an agreement between a simple deconvolution model and some laboratory measurements.

Acknowledgments: This study is performed at Jet Propulsion Laboratory (JPL), under contract with NASA and is funded by the NASA Postdoct. Program led by OakRidge Associated Universities.

REFERENCES

[1] P. Helfenstein et al. The lunar opposition effect. Icarus **128** (1997).

[2] B. Hapke. Bidirectional Reflectance Spectroscopy 5. The coherent backscatter opposition effect and anisotropic scattering. Icarus **157** (2002).

[3] M. I. Mishchenko. The angular width of the coherent back-scatter opposition effect - an application to icy outer planet satellites. Astrophys. and Space Sci. **194** (1992).

[4] Yu. G. Shkuratov et al. Opposition effect from Clementine data and mechanisms of backscatter. Icarus **141** (1999).

[5] P. Helfenstein et al. Galileo observations of Europa's opposition effect. Icarus **135** (1998).

[6] E. Déau, et al. Sunshine on the rings: the opposition effect seen at high resolution with Cassini-ISS. BAAS **38** (2006).

[7] A. K. Pierce and J. H. Waddell. Analysis of limb darkening observations. Memoirs of the Royal Astron. Soc. **63** (1961).

[8] Y. Kawata and W. M. Irvine. Models of Saturn's rings which satisfy the optical observations. In: *Exploration of the planetary system* (1974).

[9] S. Kaasalainen et al. Comparative study on opposition effect of icy Solar System objects. JQSRT **70** (2001).

[10] D. Hestroffer and C. Magnan. Wavelength dependency of the Solar limb darkening. Astr. and Astrophys. **333** (1998).

[11] E. Déau et al. The opposition effect in the outer Solar system: A comparative study of the phase function morphology. Planet. and Space Sci. **57** (2009).

[12] M. S. Bobrov. Physical properties of Saturn's rings. In: *Surfaces and Interiors of Planets and Satellites* A. Dollfus (ed.) (1970).

[13] V. Psarev et al. Photometry of particulate surfaces at extremely small phase angles. JQSRT **106** (2007).